

## 2. Study area

### 2.1 Geologic and geographic context

Regional landscape and topography is characterized by a combination of various geological settings, dominated by the geological provinces of the Appalachians and the St. Lawrence Platform (Figure 2). Although both geologic provinces are primarily sedimentary in origin, the Appalachians are highly deformed and slightly metamorphosed whereas the St. Lawrence Platform has undergone almost no deformation.

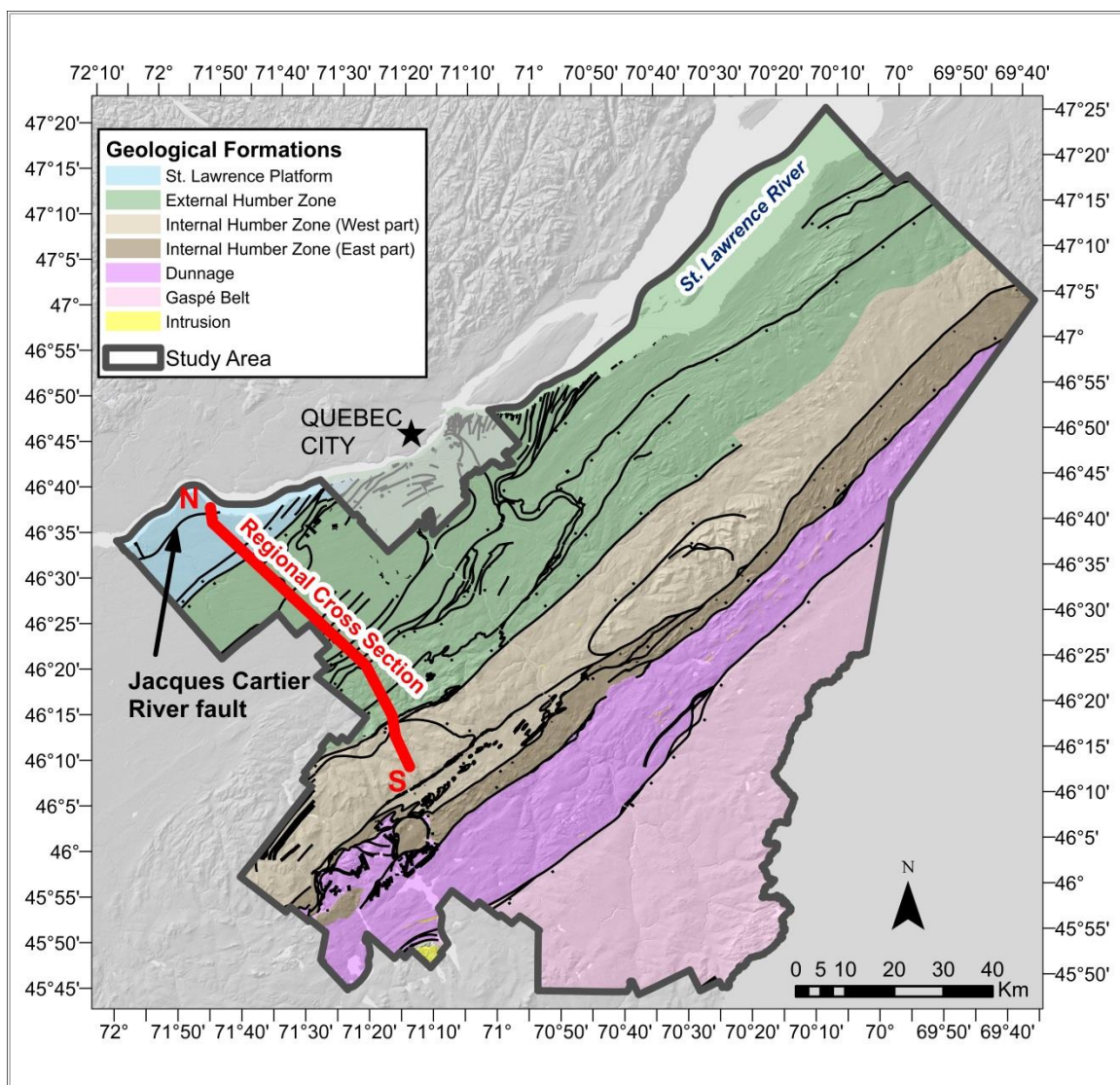


Figure 2 Regional geology of the Chaudière-Appalaches region, modified from Lefebvre et al. (2015)

Situated to the south of the study, the Appalachians are the remains of a weathered mountain range and are characterised by a hilly terrain. At the southernmost limit of the study area, the Gaspé Belt, a sedimentary basin which formed following the Taconian orogeny, sits on an oceanic sedimentary and volcanic basin called the Dunnage zone (St-Julien & Hubert 1975). The latter is followed to the north by the Humber zone which formed within a passive continental margin and is composed of carbonates, sandstones and shales (Lavoie 2002). Furthermore, the Appalachian region is marked by granitic intrusions forming small mountains, including the Petits Monts Mégantic and the Monts Notre Dame mountains (Figure 1) reaching elevations up to 850 and 1000 meters, respectively (Slivitzky & St-Julien 1987). The intrusions are surrounded by a belt of small hills, which are bordered to the south by the Appalachian plateau and to the north by a foothill area that marks the junction with the sedimentary plains of the St. Lawrence Lowlands (Slivitzky & St-Julien 1987). With a history of high tectonic activity, the Appalachian region is marked by the presence of lineaments oriented NE-SW which manifest primarily in the form of major faults (Lefebvre et al. 2015; Caron 2012).

In the northernmost part of the study area, the St. Lawrence Platform consists of a sedimentary succession sitting unconformably on the base of the Canadian Shield (Globensky 1987). Due to tectonic compression, normal faults mark the gradual lowering of the sedimentary sequence, which plunges below the Appalachian Basin (Castonguay et al. 2010) as shown in Figure 3.

The Cambrian-Ordovician sedimentary sequence of the St. Lawrence Platform is a typical marine transgression-regression sequence resulting from the opening and closing of the Iapetus Ocean. From bottom up, the sequence begins with the Potsdam Group, a poorly cemented sandstone formation becoming well cemented in its upper portion (Cloutier et al. 2006). Above this formation sits the commonly named carbonate platform which is separated into four groups. First, the Beekmantown is composed of dolomitic sandstone layers becoming pure dolostone and, near the top, dolomitic limestone. The Beekmantown is followed by the Chazy group, a clayey and sandy limestone, the Black River Group, a limestone interbedded with sandstone, and finally the Trenton group, a clayey limestone interbedded with shales (Séjourné et al. 2013; Cloutier et al. 2006). The increase in the ratio

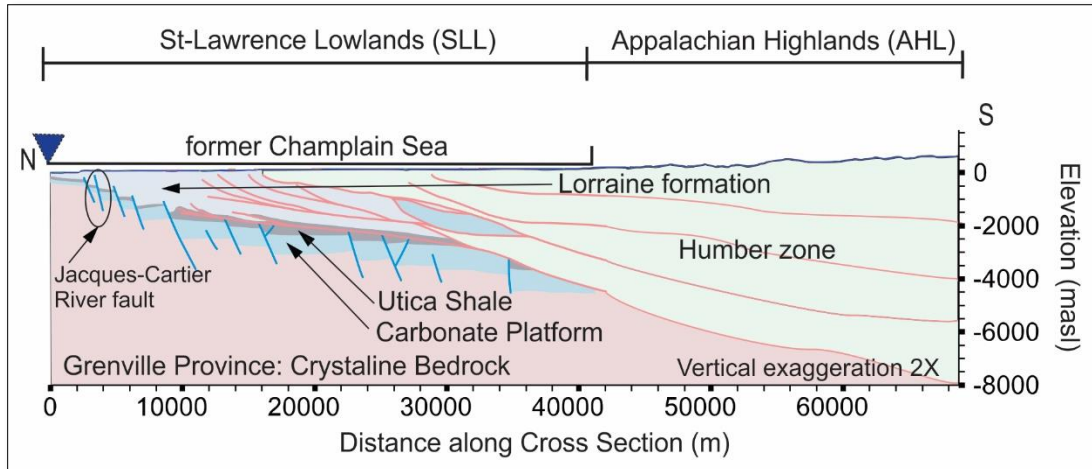


Figure 3 Geologic north-south cross-Section (see Figure 2 for location), geology based on Séjourné et al. (2013)

of shale interbeds to limestone layers marks a gradual transition towards the Utica Shale. At depths ranging from 800 to 3000 meters, the Utica Shale, which can be considered as marl due to its high carbonate content, is particularly enriched in natural gas and is of economic interest in the region (Lavoie et al. 2014; Bordeleau et al. 2015; Thériault 2012). The overlying Lorraine group, composed of silty shales with mostly non-calcareous sediments interbedded with fine sandstone and clayey siltstones (Thériault 2012) is the top formation of the St. Lawrence Platform sedimentary succession over most of the study area. In this study, *St. Lawrence Platform* refers to the geologic sequence composed of the Carbonate Platform, the Utica Shale and the Lorraine Formation while the *St. Lawrence Lowlands* refers to the relatively flat physiographic region which was formerly covered by the Champlain Sea (Figure 3).

Many past studies have identified the regional aquifer as being located in the uppermost portion of the bedrock where fracture density is highest (Lefebvre et al. 2015; Benoît et al. 2014; Ladevèze et al., 2016). Major faults could also represent areas where the level of fracturing could be relatively high, although the role of these faults on the regional flow system is not clear.

As the study area is generally covered with till deposits of various thicknesses and assemblies, the nature of the till units defines the degree of confinement of the bedrock aquifer. In the Appalachians, surficial sediments are thin or non-existent, therefore unconfined conditions prevail for most of the fractured bedrock aquifer, with the exception

of valleys where the aquifer is generally semi-confined (Lefebvre et al. 2015). Moreover, glaciation-deglaciation processes, the presence of the Champlain Sea approximately 10,000 years ago, and the formation of post-glacial lakes and shorelines, led to heterogeneous deposits with varying proportions of sand and silt. These sediments together with alluvial deposits represent significant infiltration pathways when directly in contact with the bedrock aquifer. On the other hand, scattered silt and clay sediments, deposited at the bottom of stagnant water bodies following glacial retreat, prevent recharge and are responsible for the accumulation of organic material (Lefebvre et al. 2015). These low-permeability deposits are present mostly within the area formerly covered by the Champlain Sea, specifically in the northwestern area of the St. Lawrence Lowlands (Figure 1). This region is further characterized by significant peatland coverage. Many wetlands in the area were formed over sediment deposits having strong aquifer potential and thus play a role in buffering the effect of seasonal recharge on groundwater levels (Bourgault et al. 2017).

## **2.2 Regional Piezometry**

In terms of regional groundwater flow a semi-regional groundwater divide line can be drawn across the Appalachian Highlands (Figure 4). Because of its prominent elevation as well as its limited or negligible surficial sediment cover, the Appalachian region can be considered a recharge area while the St. Lawrence River, marking the northern boundary and the lowest point of the study area, represents the regional flow outlet (Figures 4 and 5). Streams and rivers within the numerous sub-basins also act as local discharge areas, particularly since the highly fragmented terrain of the Appalachians forms a dense hydraulic network (Figure 4). The extent and contribution of regional flow to the basin-scale water budget is not yet well defined. However, the conceptual groundwater flow system of the Chaudière-Appalaches region appears to fit Tóth's (1963) concept of nested groundwater flow, in which local flow regimes are embedded within larger intermediate or regional flow regimes (Figure 5).

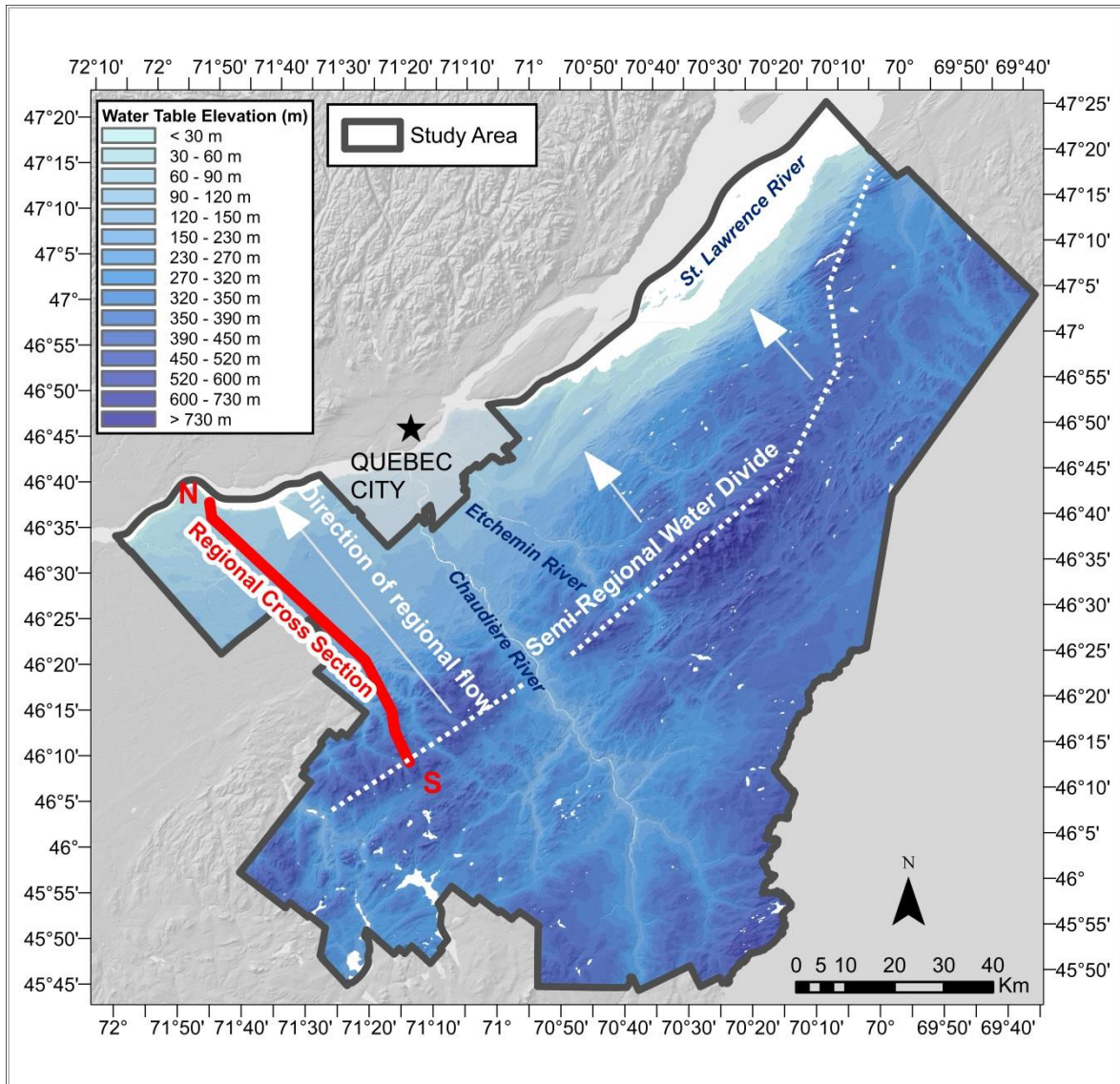


Figure 4 Water table elevation with respect to average sea level (m), modified from Lefebvre et al. (2015)

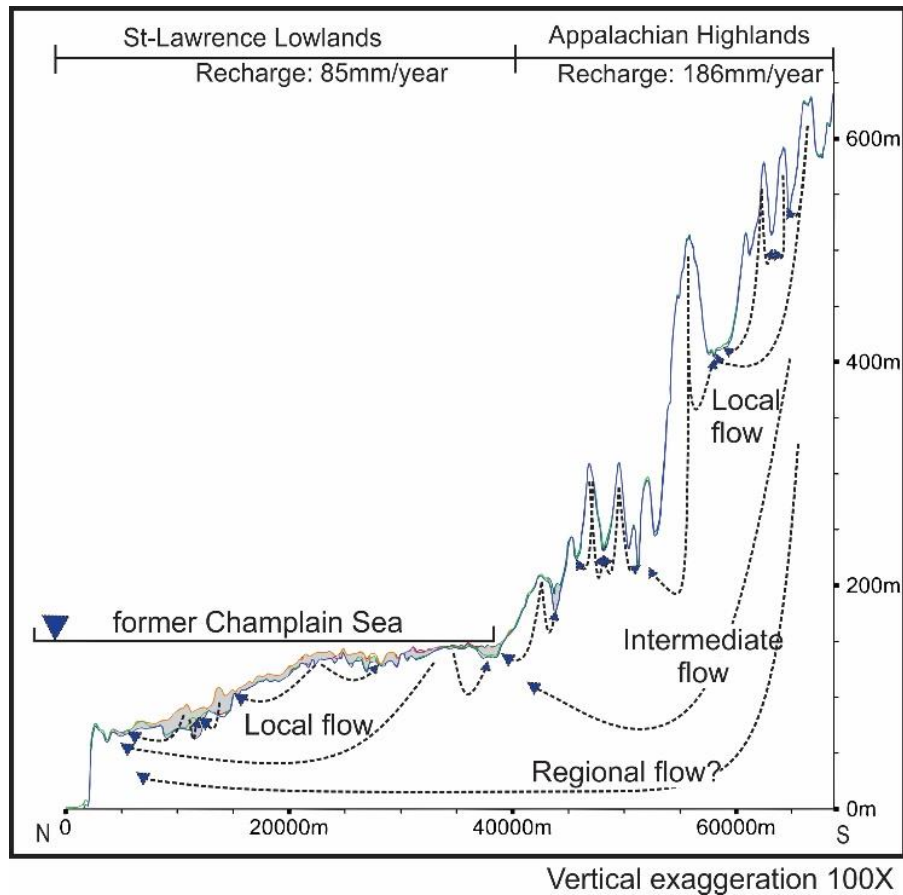


Figure 5 North-south regional cross-Section of the study area showing conceptual model of regional flow

Total precipitation over the study area is estimated to be 1149 mm/year, with an average of 166 mm/year of recharge reaching the fractured rock aquifer (Lefebvre et al. 2015). Spatial distribution of recharge is, however, highly variable. In the St. Lawrence Lowlands, areas covered with thick layers of fine sediments can receive less than 15 mm/year whereas rock outcrop areas can receive more than 300 mm/year. In the Appalachian Highlands, where the surficial sediments are fairly thin and permeable, aquifer recharge tends to be higher, varying from 100 mm/year to more than 300 mm/year. Additional studies on specific watersheds within the study area have reported overall recharge rates to the bedrock aquifer of between 27 mm/year and 38 mm/year (Benoît et al. 2014 and L'Heureux 2005, respectively). Discrepancies between recharge values could be attributed to the spatial variability of the bedrock recharge.

## 2.3 Geochemical Setting

### 2.3.1 Major Ion Chemistry

The chemical composition of a groundwater sample holds a remarkable amount of information on the path taken by groundwater (Appelo & Postma 2004; Clark and Fritz 1997; Hounslow 1995). As recharge water enters the subsurface and flows downgradient, its interactions with the minerals, gases and, to some extent, any living organisms along its path, will change the water's chemical composition (Tóth 1999; Cloutier et al. 2008).

Benoît et al. (2014) and Lefebvre et al. (2015) carried out a thorough analysis of the regional groundwater geochemistry for the Chaudière River watershed and the Chaudière-Appalaches region, respectively. The first 155 groundwater samples analysed by Benoît et al. (2014) were included in the subsequent geochemical analysis performed by Lefebvre et al. (2015) thus only the major ion water groups defined in the second study are discussed in this Section. Lefebvre et al. (2015) collected an additional 200 samples and classified a total of 355 water samples, collected mostly from residential wells (approximately 60 m deep) across the study area, into seven geochemical composition groups based on the relative proportions of their major ions. From the seven groups, three were considered as resulting from anthropogenic contamination and four were retained as natural water types, one of which is present only in a small part of the study area and thus was not included in the regional geochemical analysis (Figure 6).

The three main natural water types identified in the study area are classified as follows:

Group 1 (G1): Water of type Ca-HCO<sub>3</sub>, generally associated with young recharge waters.

Group 2 (G2): Water of type Na-HCO<sub>3</sub>, typically evolved from Ca-HCO<sub>3</sub> waters which have undergone ion exchange in the subsurface in which Ca<sup>2+</sup> ions were exchanged for Na<sup>+</sup> ions.

Group 3 (G3): Water of type Na-HCO<sub>3</sub>/Na-Cl, considered as highly evolved. High Na<sup>+</sup> and low Ca<sup>2+</sup> concentrations result from ion exchange and an elevated Cl<sup>-</sup> concentration is likely to be associated with the dissolution of salts. The origins of the chloride ions are discussed in later Sections.

For reference and comparison, four additional water types related to the study site were added to the Piper diagram: 1) the composition of a typical seawater sample (Hem 1985), 2) the composition of Sample S77 considered as Champlain Sea seawater (Cloutier et al. 2012), 3) a sample from the deepest observation well over the study area (Bordeleau et al. 2015), as well as 4) the composition of brines collected in the Cambrian-Ordovician sedimentary formation lying below the Utica Shale in the Bécancour area located to the west of the study area (Pinti et al. 2011).

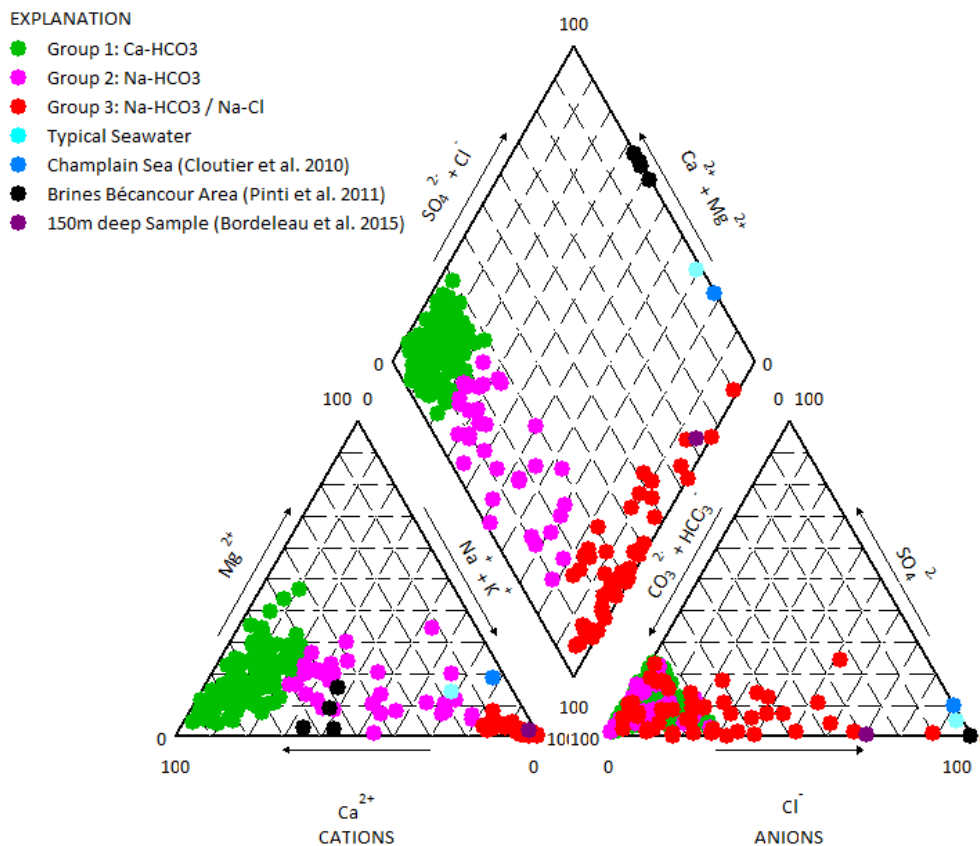


Figure 6 Piper diagram of natural water types found in the study area

The spatial distribution of the major ion water groups is consistent with the conceptual flow model discussed earlier (Figure 5). Water from group G1, associated with recharge water, can be found across the study area but is primarily found in the Appalachian Highlands, a region presumably characterized by local flow systems (supported by the geochemistry) which would imply rapid transit times. On the other hand, the dominant water type across

the St. Lawrence Lowlands is water from the more evolved group G3, implying that these samples would have had time to undergo geochemical changes. This suggests that the sampled groundwater in the St. Lawrence Lowlands has likely traveled over a longer distance and is relatively older. Water in group G2, which has undergone some level of ion exchange, is also mostly found in the St. Lawrence Lowlands. Travel times for this water group are expected to be longer than those of group 1 and shorter than those of G3.

### **2.3.2 Evidence of Geochemical Processes**

Major ion analysis of waters across the study area identified three dominant geochemical processes in the region: carbonate dissolution, ion exchange and mixing. Moreover, the proposed conceptual groundwater flow model suggests a potential input of deep fossil brines to near-surface waters, supporting the hypothesis of mixing of fresh waters and brines.

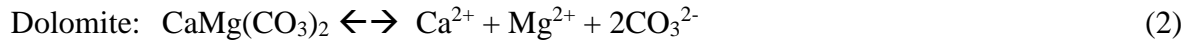
#### **2.3.2.1 Dissolution of carbonates**

Mineral dissolution is controlled by the availability of the dissolving minerals (reactants) and the solubility of the mineral (reaction rate) (Freeze and Cherry, 1979). Since the most soluble minerals, such as halite, can easily be leached away, areas with rapid renewal of water, such as recharge areas, are generally left with the slower dissolving minerals such as carbonates (Freeze and Cherry, 1979). For the present study, carbonate minerals are of particular interest since they not only have a low solubility but they are also present in the study area as 1) the main building blocks of the sedimentary St. Lawrence Platform, 2) components of the till overburden resulting from the movement of glaciers from the St. Lawrence Lowlands towards the Appalachians and 3) to a certain extent, present as cementing mineral in the rocks and fractures of the Appalachian rock formations.

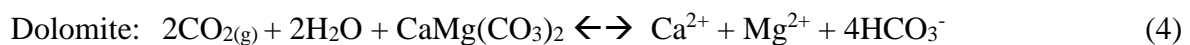
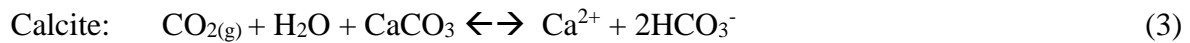
As noted by Freeze and Cherry (1979), only a small or insignificant amount of carbonate minerals can be sufficient to create saturated conditions and influence groundwater chemistry. Thus, across our study area, carbonate dissolution is inevitably taking place early along the flow path; during and soon after recharge. This is indicated by the presence

of G1 water, with major ions  $\text{Ca}^{2+}$  and  $\text{HCO}_3^-$ , signifying that dissolution of carbonate minerals has occurred through either the surficial sediments or shallow bedrock.

The equilibrium dissolution-precipitation reactions of the two most common carbonate minerals, calcite and dolomite, are given as follows:



When water enters the subsurface it first migrates through the unsaturated soil zone, where groundwater equilibrates with carbon dioxide (given off through root respiration and the decay of organic matter) to  $\text{pCO}_2$  levels that are higher than that of the atmosphere (Freeze and Cherry, 1979; Appelo and Postma 2005). Appelo and Postma (2005) point to  $\text{pCO}_2$  levels in the active soil zone ranging from the atmospheric value of  $10^{-3.5}$  atm to as high as  $10^{-1.5}$  atm. Dissolution of gaseous  $\text{CO}_2$  into water produces excess  $\text{H}^+$  ions, which at a pH of less than 8.3, bind to  $\text{CO}_3^{2-}$  ions to produce  $\text{HCO}_3^-$  which drives the dissolution of calcite and dolomite (Freeze and Cherry, 1979). The equilibrium dissolution-precipitation reactions then become:



Water is considered to be in an open system when it is in equilibrium with “soil zone”  $\text{CO}_2$ . In this case,  $\text{pCO}_2$  stays constant while carbonate minerals dissolve until equilibrium is reached. However, if the system is closed and therefore not receiving  $\text{CO}_2$  input from the soil zone,  $\text{pCO}_2$  will decrease until equilibrium is reached.

In Figure 7.A the carbon, calcite and dolomite equilibrium lines represent a pure water sample at an average temperature of 9.6 °C equilibrated using PHREEQC version 3 (Parkhurst and Appelo 1999) with  $\text{CO}_{2(\text{g})}$ ,  $\text{CO}_{2(\text{g})}$  and calcite, and  $\text{CO}_{2(\text{g})}$  and dolomite, respectively. Arrows in Figure 7 show the dissolution path in open and closed systems. The distribution shows that most samples from G1 have not yet reached calcite and dolomite equilibrium while samples from G2 and G3 appear to be saturated or supersaturated with respect to dolomite.

The final control on the dissolution of carbonate minerals is not their availability but their solubility which, for calcite and dolomite, is inversely dependant on temperature; dolomite becoming progressively more soluble than calcite with decreasing temperature (Szramek et al. 2007). At a temperature of approximately 10 °C, because of the relative solubility between the minerals, calcite might reach equilibrium and become supersaturated while dolomite remains undersaturated (Szramek et al. 2007). Furthermore, Freeze and Cherry (1979) state that in North America, supersaturation can result from the temperature gradient in the soil during spring. During spring recharge, dissolution occurs at low temperatures under open conditions. But, at a few meters of depth, temperatures can be several degrees higher than at the surface, leaving the water supersaturated in calcite and dolomite. The temperature difference between the recharge zone and the aquifer could explain the calcite supersaturation of water samples from G2 and G3 observed in Figures 7.A, 7.C and 7.D.

Figures 7.A and 7.C also confirm that by having  $p\text{CO}_2$  levels lower than atmospheric levels, all samples from G3 were likely collected from closed system conditions in which the carbon dioxide initially present in the system was consumed by the dissolution of carbonates until equilibrium. Conversely, samples from G1 and G2 have  $p\text{CO}_2$  levels corresponding to that of the soil zone, thus indicating that these samples either reached equilibrium under open conditions or that  $p\text{CO}_2$  in the soil zone was initially high.

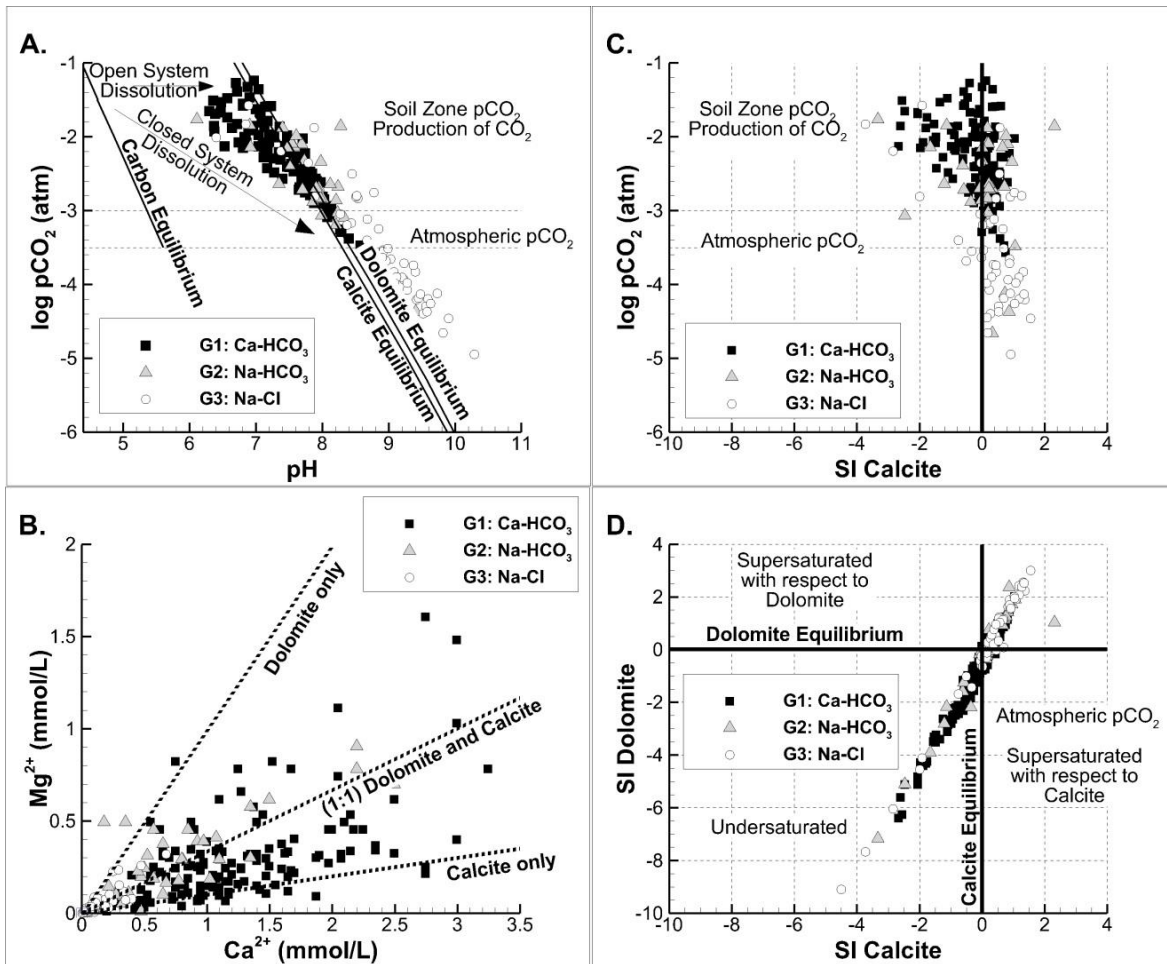


Figure 7 Evidence of carbonate dissolution in the C-A study area: a) Calcite and dolomite equilibrium with respect to pH and partial pressure of CO<sub>2</sub>; b) Ca<sup>2+</sup> and Mg<sup>2+</sup> ratios of dissolving carbonates, c) Saturation of calcite with respect to partial pressure of CO<sub>2</sub>, and d) Saturation of calcite with respect to dolomite.

Freeze and Cherry (1979) state that despite laboratory experiments showing that calcite equilibrium can be reached within hours or days, field rates are often slower. Nevertheless, carbonate dissolution reactions can be considered as being fairly rapid over a regional-scale flow system. Thus, samples that have not reached calcite and dolomite equilibrium, mainly those from G1, can be considered as being recently recharged water. Furthermore, high pCO<sub>2</sub> levels can also indicate that the aquifer has a shallow circulation zone keeping the system in open conditions or that the flow distance between recharge and discharge zones is short. The large range of pCO<sub>2</sub> and pH across the samples testifies to the variability of recharge conditions and state of evolution among the water samples.

In this context, the low final pCO<sub>2</sub> levels of waters from G3 relative to G1 could indicate that G3 waters were recharged under lower initial soil pCO<sub>2</sub> levels.

For a system in which the only carbon sources are dissolved carbon dioxide and carbonate minerals, stoichiometry can be used to derive the expected ratios between the concentrations of dissolved inorganic carbon (DIC) and Ca<sup>2+</sup> ions for minerals dissolving in various proportions (Figure 8). The data show that water from group G1 has DIC/Ca<sup>2+</sup> ratios corresponding to the dissolution of calcite and dolomite, while samples from G2 and G3 are affected by a process removing Ca<sup>2+</sup> ions from the system (Figure 9a).

### 2.3.2.2 Cation exchange

Cloutier et al. (2010), Lefebvre et al. (2015) and Benoît et al. (2014) identified Ca<sup>2+</sup>/Na<sup>+</sup> ion exchange as another important geochemical process in the study area. Ion exchange is described as the process by which one ion is replaced by another ion at the surface of a solid (Appelo and Postma 2005). In Chaudière Appalaches, this reaction can be described through the following equation:



In this case, when considering the Na<sup>+</sup> ions as having been exchanged for Ca<sup>2+</sup> (Figure 8B), water samples from groups G2 and G3 appear to be strongly affected by the cation exchange process (Figures 9A and 8B).

As a side note, it is worth noting that when accounting for ion exchange, the ratio of dissolved dolomite to calcite indicates that calcite is the main dissolving mineral and that water from G3 is affected by yet another process adding Na<sup>+</sup> ions to the system (Figure 8B).

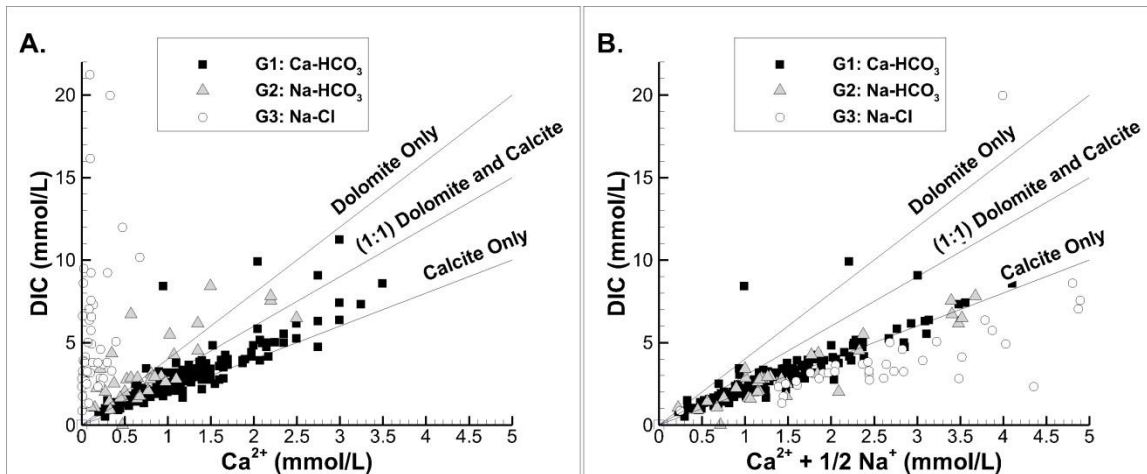


Figure 8 Expected ratios between the concentrations of DIC and Ca<sup>2+</sup> ions for minerals dissolving in various proportions: a) DIC with respect to Ca<sup>2+</sup> ions b) DIC with respect to measured Ca<sup>2+</sup> ions and exchanged Ca<sup>2+</sup> ions, assuming all Na<sup>+</sup> ions are from Ca<sup>2+</sup>/Na<sup>+</sup> ion exchange

Lefevre et al. (2015), Appelo and Postma (2005) and Cloutier et al. (2010) attribute waters of type Na-HCO<sub>3</sub><sup>-</sup> (group G2) to the process of aquifer freshening. During the salinization process, Na<sup>+</sup> ions, being abundant in seawater, bind to ion exchange sites in the aquifer. As fresh water with abundant Ca<sup>2+</sup> ions replaces the salty pore water, the new dominant ion in solution will replace the ions at the exchange sites, in this case releasing Na<sup>+</sup> ions. The final step of freshening is when Na<sup>+</sup> ions have been completely replaced by Ca<sup>2+</sup> and the water returns to Ca<sup>2+</sup>-HCO<sub>3</sub><sup>-</sup> type. The time required for Na<sup>+</sup> to be flushed from the system can provide a relative estimate of the groundwater velocity and thus the age of groundwater. For instance the presence of Na-HCO<sub>3</sub> type water indicates that seawater has been completely replaced by fresh water in the aquifer so that it is younger than at the beginning of the freshening event.

As Cloutier et al. (2010) states, three conditions are required for cation exchange to occur as described by Equation (5). First, Ca<sup>2+</sup> ion concentrations need to be high enough to displace Na<sup>+</sup> ions. This condition is met through the dissolution of carbonates. Then, the aquifer must have a high cation exchange capacity (CEC), which is dependent on the specific surface area and the clay mineral, organic matter and oxide or hydroxide content (Appelo and Postma 2005). According to Cloutier et al. (2010), in the St. Lawrence Lowlands, sites with a high CEC can be found either in rock aquifers or in overlying confined aquifers. In the Chaudière-Appalaches study area, fractured sedimentary rock

formations of the St. Lawrence Platform are dominated by organic-rich black shales (Lavoie et al. 2016) and clay minerals in these formations can act as cation exchange sites (Cloutier et al. 2010). Another possibility is for cation exchange to occur on the clay minerals within till aquitard confining units (Cloutier et al. 2010). Finally, for exchange to occur, exchange sites need to be charged with  $\text{Na}^+$  ions, i.e. the aquifer needs to have been in contact with water having  $\text{Na}^+$  as its major cation.

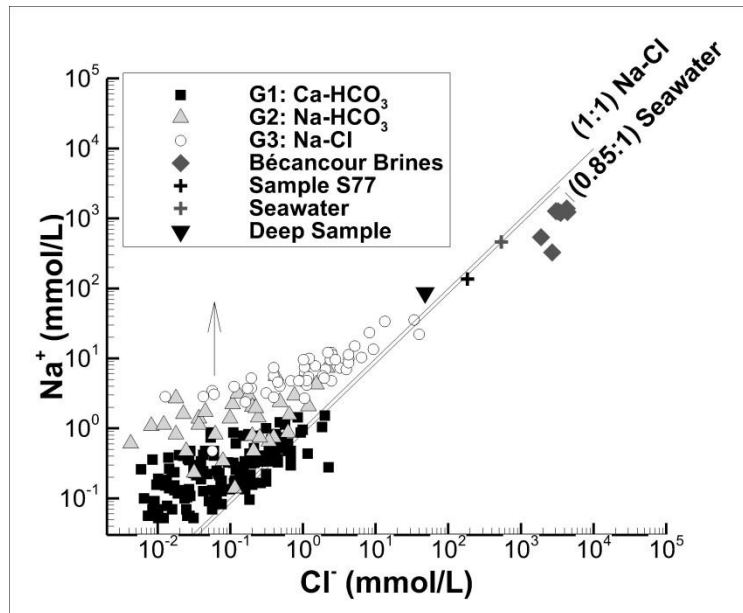


Figure 9 Na/Cl ratios indicating mixing and ion exchange

Cloutier et al. (2010), Beaudry (2013) and Lefebvre et al. (2015) postulate that during invasion of the Champlain Sea, saline water also infiltrated into the underlying fractured aquifers. Flushing of these waters with freshwater precipitation would have occurred following retreat of the sea. The source of groundwater salinity is thus attributed to seepage of Champlain seawaters composed of a mixture of fresh and glacial melt water (66%) mixed with seawater (34%) (Cloutier et al. 2010). Evidence of groundwater freshening through the emergence of  $\text{Na-HCO}_3^-$  water type was also noted in similar sedimentary aquifers across North America and Europe (Siegel 1991; Pärn et al. 2016; McIntosh and Walter 2006; Ferguson et al. 2007). These aquifers remained continental and glacial melt waters formed fresh lakes. The salinity source in these areas is thus attributed to marine formation waters (Siegel 1991; Pärn et al. 2016; McIntosh and Walter 2006; Ferguson et al. 2007). In the context of the Chaudière-Appalaches region, both the Champlain Sea and

formation water are plausible sources of the initial aquifer salinity and place the maximum ground water ages of group G2 water to different eras.

### 2.3.2.3 Mixing

The large range of  $\text{Cl}^-$  ion concentrations in the samples indicates that the rate of water replacement is likely to have occurred at variable intensities over time due to the presence of preferential pathways (rapid flushing) and stagnation zones (slow flushing) (Cloutier et al. 2012). Thus mixing with residual seawater or formation waters accounts for the high  $\text{Cl}^-$  concentrations (Benoît et al. 2014; Lefebvre et al. 2015).

Typical ratios for Na-Cl dissolution and mixing with seawater are represented in Figure 9, where the upward arrow represents cation exchange. Although affected by ion exchange, the G3 water type also results from mixing with saline waters (Figure 9). Using  $\text{Cl}^-$  ions as a conservative tracer for the saline water, the excess  $\text{Na}^+$  ions likely originate from ion exchange. Similarly, Figure 8 illustrates how the amount of exchanged  $\text{Na}^+$  cations can be calculated from the expected  $\text{Ca}^+/\text{DIC}$  ratio for the dissolution of calcite. When comparing the ions exchanged using the two methods (Figure 10A), it appears that waters from group G3 have an excess of  $\text{Na}^+$  unaccounted for by the ion exchange with respect to seawater and dissolved halite (Figure 10B).

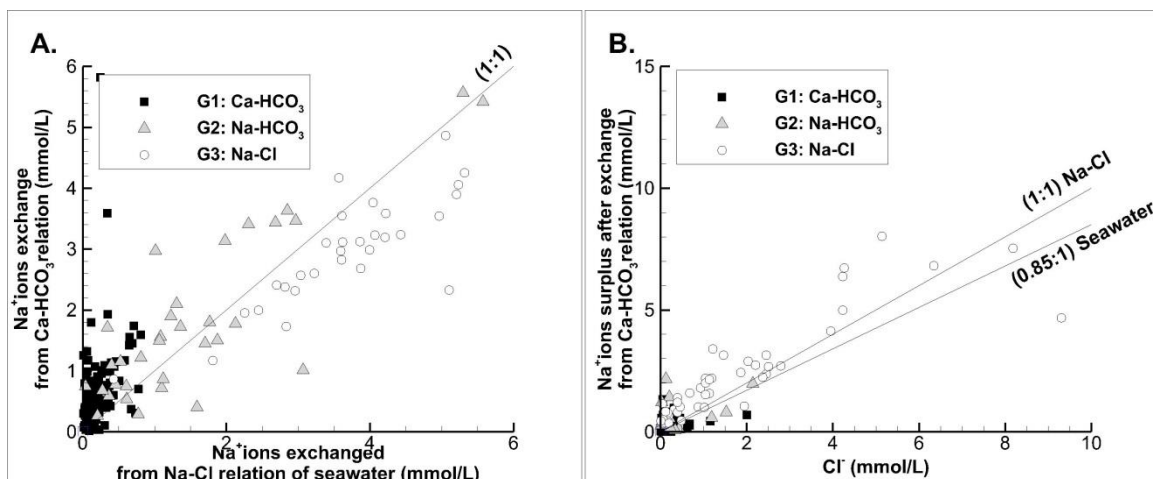


Figure 10 Comparison of  $\text{Na}^+$  ions exchanged using  $\text{Cl}^-$  as a conservative tracer with the excess  $\text{Na}^+$  obtained from the dissolution of calcite: a)  $\text{Na}^+$  ions exchanged calculated from calcite dissolution with respect to  $\text{Na}^+$  ions exchanged calculated from surplus of seawater Na-Cl ratio, b)  $\text{Na}^+$  ions surplus after ion exchange with respect to  $\text{Cl}^-$  concentration in samples

The possible natural sources of excess  $\text{Na}^+$  ions, other than seawater mixing and ion exchange are: water-rock interaction along the flowpath and mixing with formation waters (Hem 1985). The specific geochemistry of formation waters of the fractured rock aquifer is unknown. However, considering the marine origin of the sedimentary formation, it is expected to have a  $\text{Na}^+/\text{Cl}^-$  ratio close to that of seawater at the time of sedimentation. Alternatively,  $\text{Na}^+$  ions can also be associated with silicate mineral dissolution (Appelo and Postma 2005; Freeze and Cherry 1979; Hem 1985), the kinetics of which would require residence times of hundreds of thousands of years under the chemical conditions found over the study area (Pärn et al. 2016).

Similarly, the concentrations of conservative ions  $\text{Li}^+$  and  $\text{Br}^-$  increase with increasing  $\text{Cl}^-$  concentrations and the ratios of  $\text{Li}^+$  to  $\text{Cl}^-$  and  $\text{Br}^-$  to  $\text{Cl}^-$  (Figures 11 and 12) also exceed those of seawater for group G3 samples, suggesting that G3 water has a relatively long residence time.  $\text{Li}^+$  to  $\text{Cl}^-$  ratios exceeding the seawater composition are also observed in G1 and G2 samples, suggesting  $\text{Li}^+$  ions might have been released by ion exchange. However,  $\text{Br}^-$  to  $\text{Cl}^-$  ratios show that while G1 waters tend to be depleted in  $\text{Br}^-$ , some G3 samples are enriched which supports the hypothesis of long residence times.

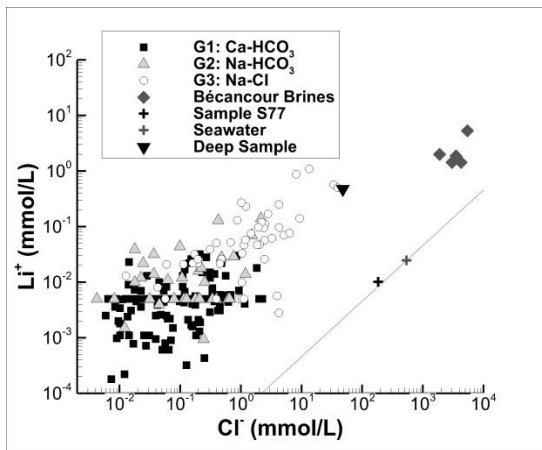


Figure 11  $\text{Cl}^-$  and  $\text{Li}^+$  concentrations

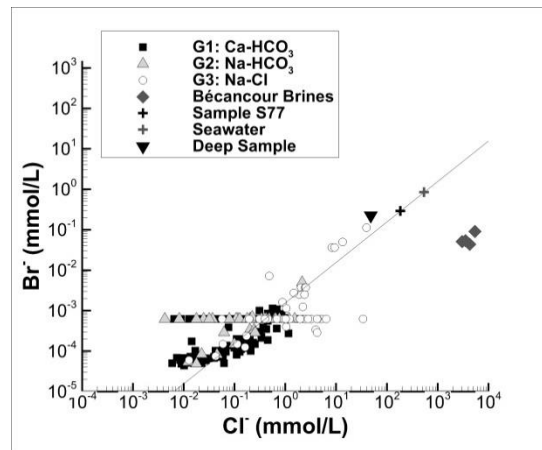


Figure 12  $\text{Br}^-$  and  $\text{Cl}^-$  concentrations

In addition, Saby et al. (2016) looked at the link between groundwater quality, regional geology and residence times in the St. Lawrence Lowlands. Focusing on the Nicolet watershed, located west of the Chaudière-Appalaches region, they found that long

interaction times between groundwater and the Ordovician rocks from the St. Lawrence platform and the Appalachian mountains were likely to be an important factor in the release of Ba, F, Fe and Mn ions which were found in anomalous concentrations in residential wells.

Furthermore, they also looked at  $^3\text{H}/^3\text{He}$  and  $^{14}\text{C}$  isotopes, and found that their samples were composed of a mixture of young water less than 60 years of age with water several thousands of years old that likely infiltrated the Cambro-Ordovician aquifers by subglacial recharge. Supporting the hypothesis of mixing, Vautour et al. (2015) suggest that there are two different water mixtures in the St. Lawrence Lowlands. The first is a mixture of modern infiltration with fossil water from the shallow fractured bedrock aquifer which would have resulted from the infiltration and flushing of the Champlain Sea. The second water mixture is likely a blend between an evolved groundwater which recharged in the Appalachian area and fossil groundwaters from the fractured bedrock aquifer that predate the Champlain Sea invasion episode. In concordance with the conceptual flow model presented in Section 2.2, this suggests that a portion of the groundwater recharging the Appalachians travels along a regional flow path, mixes with fossil water and emerges in the St. Lawrence Lowlands.

The hypothesis of the emergence of a regional flow system in the St. Lawrence Lowlands is also corroborated by Bordeleau et al. (2017) who collected two water samples, in the Saint-Édouard-de-Lotbinière area, near the northern end of the discussed regional flow path, at a depth of 48 m below the surface without disturbing the water column in the well and dated the samples over 1.5 Ma using chlorine-36 isotopes. Based on the hypothesis that these samples could contain water from deeper horizons, Bordeleau et al. (2017) estimated that these samples contained 4% and 7% brine. The study concluded that faults present in the Saint-Édouard-de-Lotbinière study area could act as preferential pathways for the migration of formation waters.

### 2.3.3 Radiocarbon ages

Some of the groundwater samples collected over the CA study area, 37 by Lefebvre et al. (2015), 10 by Benoît et al. (2014) and 18 by Bordeleau et al. (2017), were also analyzed for isotopes aiming specifically at characterizing residence time (tritium, radiocarbon). In order to gain a better understanding of the characteristic time scales associated with the hydrogeological setting of the study area, the interpretation of the groundwater residence times based on carbon isotopes attributed to these samples is explored in this Section.

The radioactive form of carbon,  $^{14}\text{C}$ , is produced in the upper atmosphere by cosmic radiation and enters the hydrosphere under its oxidized form,  $^{14}\text{CO}_{2(\text{g})}$ . In an open groundwater system, the dynamic carbon cycle will maintain atmospheric  $^{14}\text{C}$  concentrations. However, when a system becomes closed to the atmosphere, radioactive decay of  $^{14}\text{C}$  can be used to measure the time elapsed since a sample entered closed system conditions (Equation 6).

$$t = -8267 \times \ln\left(\frac{A_t^{14}\text{C}}{A_o^{14}\text{C}}\right) \quad (6)$$

Where,

$t$ = time since the sample entered the closed system

$A_o^{14}\text{C}$ = initial activity of the sample

$A_t^{14}\text{C}$  = activity of a sample at time  $t$

Nevertheless, Equation 6 is only valid under two major assumptions and its application becomes problematic when different geochemical processes are affecting the sample.

The first assumption when using Equation 6 is that the system is closed to the atmosphere such that no further gain or loss of  $^{14}\text{C}$  is possible (Clark 2015). Section 2.3.2.1 presents the challenges of determining whether a sample was collected in a closed or open system. For the purpose of radiocarbon dating in the context of this study, an arbitrary level of  $\text{pCO}_2=10^{-2.5}$  atm (Appelo and Postma 2005) was chosen as the limit between samples in open and closed systems. In Figures 8.A and 8.C, this represents the level beyond which all

samples are near or over the calcite saturation limit and only the samples below this limit are considered for radiocarbon dating.

The second assumption when using radiocarbon as a dating method is that the initial concentration of the parent ( $A_0$ ) is known (Clark 2015). This can be challenging since relative  $^{14}\text{C}$  levels in the atmosphere have fluctuated over time, reaching up to 10% during the Holocene and 20 to 30% in the late Pleistocene (Clark 2015). However, the error related to the fluctuation of atmospheric  $^{14}\text{CO}_2$  levels is often negligible with respect to the errors induced by the dilution of  $^{14}\text{C}$  through various geochemical reactions occurring in the subsurface (Clark 2015).

In some studies, the  $^{14}\text{C}$  concentration of a sample identified to be from a recharge area is assumed to represent the initial activity and is assigned to a group of samples (Appelo and Postma 2005). This assumption, however, can be inaccurate since young waters may have been contaminated by the high  $^{14}\text{C}$  activity in the atmosphere during the post-bomb era and may not be representative of the conditions found at the time when the water samples were recharged (IAEA 2013). In the present study, samples from group G1 (recognised as recharge water in Section 2.3.1) and identified to be in an open system with respect to the cut-off level described above, have  $^{14}\text{C}$  concentrations between 64 and 104 pMC. Samples with concentrations above 100 pMC are representative of modern atmospheric  $^{14}\text{C}$  levels (Levin and Kromer 2004). Conversely, concentrations less than 100 pMC in the recharge area are likely to indicate that geochemical reactions are taking place during infiltration (Montcoudiol et al. 2015; IAEA 2013). Given the large range of  $^{14}\text{C}$  concentrations found in recharge zone waters in the CA study area, it is evident that a variety of reactions were affecting their radiocarbon signature. Thus, rather than using a bulk value, the initial activity of radioactive carbon should be adjusted for each sample individually. Several correction methods based on empirical models, chemical balancing, statistics and modelling have been proposed to adjust  $A_0$  to account for these processes (Han and Plummer 2016) (Table 1). The choice of correction to apply depends on the processes affecting the water samples and the information available with respect to these processes.

All conventional chemical balancing correction models require knowledge or assumptions with respect to the isotopic composition of soil  $\text{CO}_{2(g)}$  and the carbonate rock. The

carbonate rocks in the study area are of Paleozoic marine origin and can therefore be assigned  $^{14}\text{C}=0$  pMC and  $\delta^{13}\text{C}=0.0$  ‰. On the other hand, the value of  $\delta^{13}\text{CO}_{2(\text{g})}$  in the soil is derived from the decomposition of organic matter, plant root respiration and atmospheric  $\text{CO}_2$  (Gillon et al. 2012; Amundson et al. 1998) and is highly dependent on the biological and physical conditions prevailing in the recharge area which can vary seasonally (Gillon et al. 2012). In a temperate climate, dominated by C-3 plants, soil  $\delta^{13}\text{CO}_{2(\text{g})}$  is expected to be between -35‰ and -19‰ (Gillon et al. 2009). Samples categorized as being under open conditions can be used to estimate of  $\delta^{13}\text{CO}_{2(\text{g})}$  using Equation 7 (IAEA 2013):

$$\delta^{13}\text{CO}_{2(\text{g})} = \frac{1}{n} \sum_{i=1}^n \delta^{13}\text{C}_{\text{DIC}-i} + \left( \frac{\text{H}_2\text{CO}_3}{c_T} \cdot \varepsilon_{\text{CO}_{2(\text{g})}-\text{H}_2\text{CO}_3} + \frac{\text{HCO}_3^-}{c_T} \cdot \varepsilon_{\text{CO}_{2(\text{g})}-\text{HCO}_3^-} + \frac{\text{CO}_3^{2-}}{c_T} \cdot \varepsilon_{\text{CO}_{2(\text{g})}-\text{CO}_3^{2-}} \right) \quad (7)$$

Where,

$\varepsilon$  = fractionation factor

i= samples identified as being in an open system

In our study area, the average  $\delta^{13}\text{CO}_{2(\text{g})}$  of the samples categorized as being in an open system is 25.4‰ (Annex A, Table A1). Although using a single value for  $\delta^{13}\text{CO}_{2(\text{g})}$  inevitably introduces uncertainty into the age corrections by not taking into account seasonal variations of  $\delta^{13}\text{C}$  of soil  $\text{CO}_2$  (Gillon et al. 2012), in the context of this study, it represents a reasonable approximation.

Furthermore, the concentration of soil  $^{14}\text{C}$  also depends on the relative contribution of root respiration with respect to the degradation of organic matter from old or young reservoirs (Gillon et al. 2012). However, these effects are the direct result of nuclear weapons testing and are not important when dating sub-modern groundwater (Gillon et al. 2012). Assuming that the samples were recharged during the pre-bomb era, the soil  $^{14}\text{CO}_{2(\text{g})}$  can therefore be assumed to be 100 pMC (Appelo and Postma 2005).

Table 1 Conventional adjustment models accounting for geochemical reactions affecting the initial activities used for the determination of groundwater sample ages, modified from IAEA (2013) (Han and Plummer 2016; Clark and Fritz 1997)

Model								Description
	Carbonate dissolution	Soil gas dissolution	CO <sub>2</sub> - Gas aqueous exchange	Calcite - HCO <sub>3</sub> <sup>-</sup> exchange	Gypsum dissolution	Ca/Na exchange		
Fontes and Garnier <sup>a</sup>	x	x	x	x	x	x	x	<ul style="list-style-type: none"> <li>Mixing of two end members:                             <ol style="list-style-type: none"> <li>soil gas CO<sub>2</sub></li> <li>solid carbonate mineral</li> </ol> </li> <li>Partial isotopic exchange only between a part of the CO<sub>2</sub> gas and calcite mineral in a closed system.</li> <li>Reduces to the Tamers model if there is no isotopic exchange.</li> </ul>
IAEA <sup>b</sup>	x	x	x					<ul style="list-style-type: none"> <li>Isotopic mass balance in two steps:                             <ol style="list-style-type: none"> <li>equilibrium of the HCO<sub>3</sub><sup>-</sup> with the gas phase (open system);</li> <li>dissolution of solid carbonate in closed systems.</li> </ol> </li> </ul>
Evans <sup>c</sup>	x	x		x				<ul style="list-style-type: none"> <li>Accounts for isotopic fractionation during dissolution–precipitation of calcium carbonate.</li> <li>Assumes calcite to be in isotopic equilibrium with dissolved HCO<sub>3</sub><sup>-</sup>.</li> <li>Results similar to Pearson’s model.</li> </ul>
Mook <sup>d</sup>	x	x	x					<ul style="list-style-type: none"> <li>Considers partial or complete isotopic equilibration in the soil zone between CO<sub>2</sub> gas and all aqueous carbon-bearing species, including part of the dissolving carbonate mineral in open systems.</li> <li>Appropriate in systems in which reactions with carbonate minerals are not dominant.</li> </ul>
Pearson <sup>e</sup>	x							Similar to Tamers but accounts for dissolution of carbonates by using isotope mass balance relations for <sup>13</sup> C and <sup>14</sup> C in open systems.
Eichinger <sup>f</sup>	x	x		x				<ul style="list-style-type: none"> <li>Similar to Pearson model.</li> <li>Only includes isotope exchange with the solid phase in closed system.</li> </ul>
Han and Plummer (2013) <sup>g</sup>	x	x	x	x				<ul style="list-style-type: none"> <li>Revises the mass balance method of Fontes and Garnier.</li> <li>Models assume either:                             <ol style="list-style-type: none"> <li>isotopic exchange dominated by gaseous CO<sub>2</sub> in the unsaturated zone which yields similar results to the Mook model,</li> <li>isotopic exchange dominated by solid carbonate minerals in the saturated zone, which yields similar results to the Eichinger model, or</li> <li>if no carbon isotopic exchange occurs, it reduces to Tamer’s model</li> </ol> </li> </ul>
Tamers <sup>h</sup>	x	x	x					<ul style="list-style-type: none"> <li>Assumes that the initial quantity of soil zone CO<sub>2</sub> containing <sup>14</sup>CO<sub>2</sub> is diluted by dissolution of carbonates in recharge area, with no other sources or sinks of carbon in the system.</li> <li>Does not consider carbonate isotopic exchange.</li> </ul>
Extended Gonfiantini and Zuppi <sup>i</sup>	x	x	x	x	x	x	x	<ul style="list-style-type: none"> <li>Statistical approach based on the relationship between <sup>14</sup>C and δ<sup>13</sup>C.</li> <li>Applicable if <sup>14</sup>C vs. δ<sup>13</sup>C of sample form exponential curve.</li> <li>Can be used to identify outliers from the relationship between <sup>14</sup>C and δ<sup>13</sup>C data.</li> </ul>

a- Fontes and Garnier (1979), b- Salem et al. (1980), c- Evans et al. (1979), d- Mook (1976), e- Ingerson and Pearson (1964), f- Eichinger (1983), g- Han and Plummer (2013), h- Tamers (1975), i- Han et al. (2014).

Different methods used to account for various geochemical reactions in the calculation of  $^{14}\text{C}$  ages are presented in Table 1. The ages of the samples collected over the study area were estimated using each correction method (Annex A, Table A2). Discrepancies between ages calculated using different methods can be significant (Figure 13), which emphasizes the uncertainties associated with radiocarbon dating of groundwater and the importance of selecting the appropriate adjustment model.

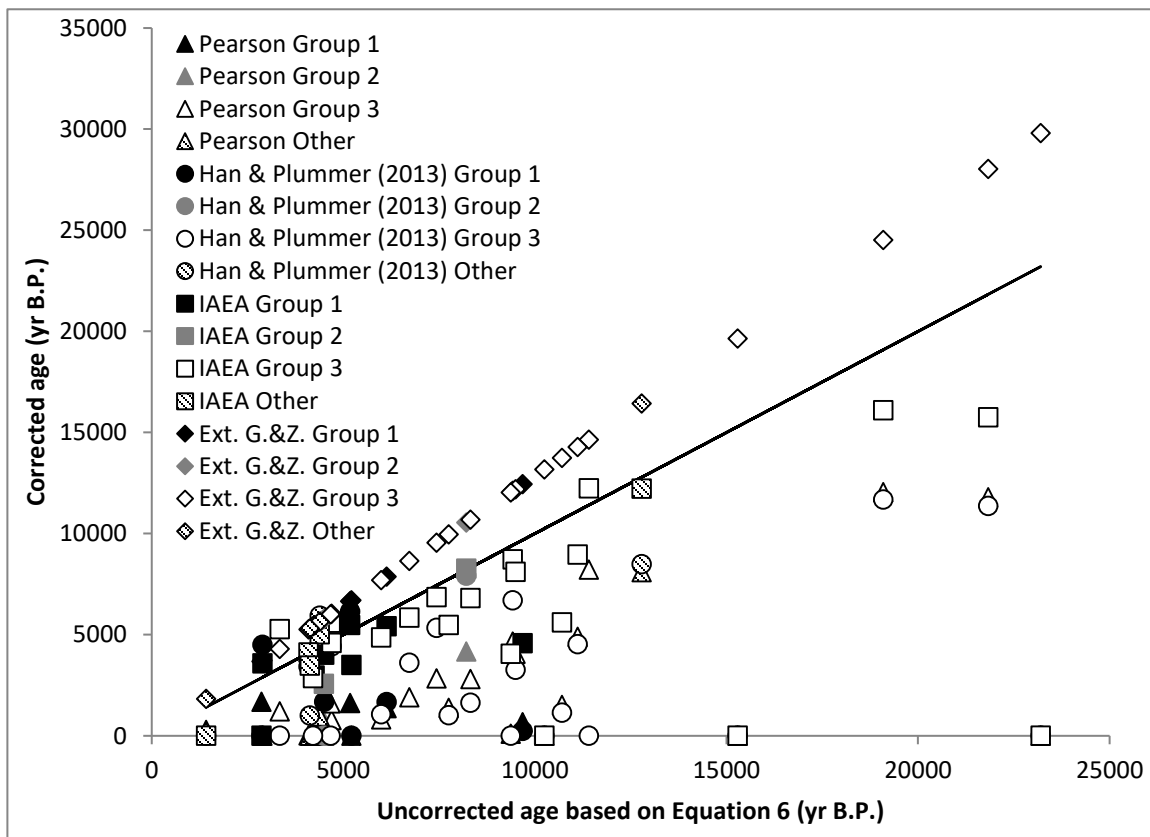


Figure 13 Comparison of radiocarbon ages calculated using various methods

In order to select the right correction method to be applied for each sample, Han and Plummer (2016) suggest a graphical methodology which allows designating the method that more accurately accounts for chemical and isotopic exchanges affecting the samples (Figure 14). On a  $^{14}\text{C}$  vs  $\delta^{13}\text{C}$  plot, the three most accurate and up-to-date correction methods (Pearson, Han and Plummer (2013) and IAEA) are each assigned  $^{14}\text{C}$  and  $\delta^{13}\text{C}$  ranges under which they should be applied to appropriately account for carbonate reactions and isotopic exchanges under open and closed conditions (Han and Plummer 2016) (Figure

14). This method was used to determine which correction method is most applicable for each sample. Results are presented in Table A2, Annex A.

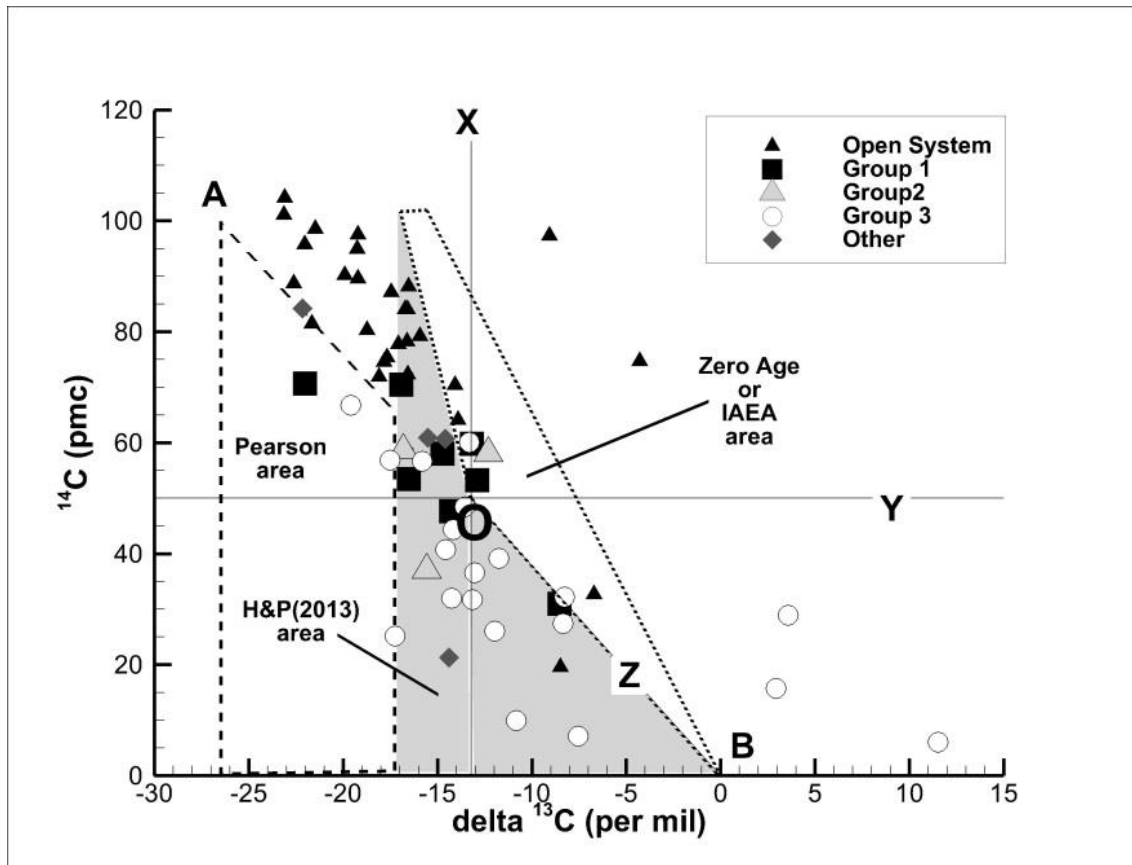


Figure 14 Carbon isotope concentrations of samples collected in the Chaudière-Appalaches region plotted on Han and Plummer's (2016) graphical interpretation of the validity of correction methods

The distribution of the sample ages obtained using Han and Plummer's (2016) methodology is consistent with the geochemical interpretation of the major ion water groups (Table 2, Figure 15). G1 waters are the youngest, having ages between 0 and 4000 years and G3 waters contain the oldest water samples, having ages ranging between 1000 and 12000 years. The maximum age of samples from G2 is 8000 years (younger than the Champlain Sea) which supports the conclusion that water type G2 results from the freshening of the aquifer. The presence of G3 samples with ages corresponding to the era of the Champlain Sea indicates that some water in the study area could have been recharged prior to or during the invasion of the post-glacial sea. However, it remains unconfirmed

whether the long residence times of G3 waters are attributed to stagnation zones, long travel paths or mixing with older waters such as formation brines.

Table 2 Distribution of radiocarbon groundwater ages estimated using Han and Plummer's (2016) method

Water Type	G1	G2	G3	Other
Total number of samples	19	9	23	15
Number of samples assumed to be in open system	11	6	3	10
Number of samples for which Han and Plummer (2016) is not applicable	1	0	3	1
Maximum age (yr B.P.)	3496	7914	11680	8489
75 <sup>th</sup> Quartile (yr B.P.)	2336	5238	5334	4686
Median Age (yr B.P.)	1676	2563	3617	2212
25 <sup>th</sup> Quartile (yr B.P.)	1644	1784	1600	994
Minimum age (yr B.P.)	242	1005	1019	959

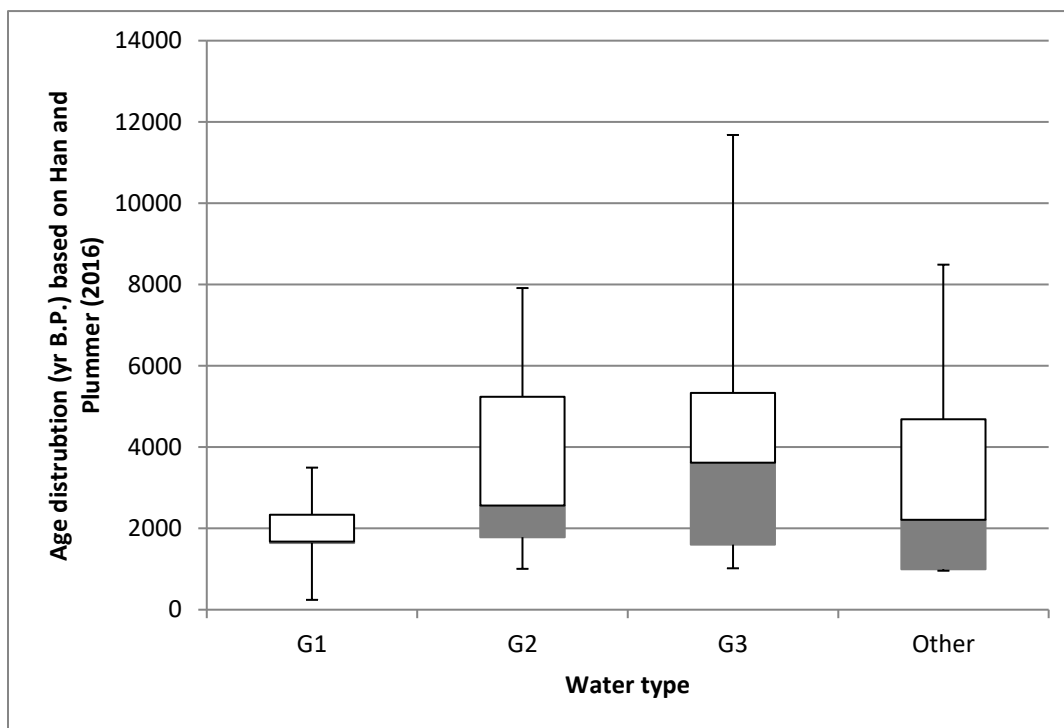


Figure 15 Distribution of radiocarbon groundwater ages estimated using Han and Plummer's (2016) method. Whiskers represent maximum and minimum values, and boxes represent percent quartiles.

Furthermore, it is important to note that while some geochemical processes are accounted for in the conventional initial activity adjustment models, others require geochemical modeling in order to accurately estimate groundwater ages.

Based on the interpretation of the St. Lawrence Lowland and Appalachian geochemistry, the main processes involved in modifying the carbon isotopic composition of groundwater in the study area in both open and closed systems are likely (1) dissolution of soil CO<sub>2(g)</sub> (2) dissolution of carbonate minerals (3) isotopic exchanges between DIC, soil CO<sub>2(g)</sub> and carbonate minerals (4) methanogenesis involving old or young organic matter and (5) mixing of different water types (Rivard et al. 2014; Lefebvre et al. 2015; Saby et al. 2016; Benoît et al. 2014; Vautour et al. 2015; Bordeleau et al. 2015; Cloutier et al. 2010; Beaudry, 2013). While the first three processes are incorporated in the conventional correction models, methanogenesis and water mixing are not, which can considerably offset apparent groundwater ages. A more accurate estimate of radiocarbon ages for samples undergoing complex reactions could be obtained through geochemical modelling. Such modelling, however, requires an in-depth knowledge of the chemical, mineralogical and isotopic conditions along the flow paths which unfortunately is not available in the context of this study. However, analysing what reactions are likely to affect each sample can give insight into the path the water has taken and can help validate corrected groundwater ages.

Han et al. (2012) suggest a graphical method to identify which geochemical reactions are affecting the samples based on the trends between  $\delta^{13}\text{C}$ ,  $^{14}\text{C}$  and DIC concentration (Figures 16 and 17). Arrows in Figures 16 and 17 identify geochemical processes affecting the samples, and the colors serve to group samples that have undergone similar reactions.

Points A and B on Figure 16.III and 17.III represent the two end members of mixing between two carbon reservoirs; soil CO<sub>2</sub> (depleted in  $\delta^{13}\text{C}$ ) and “dead” carbon ( $\delta^{13}\text{C}=0$ ).

On Figures 16 and 17, point O represents the “crossing point”, i.e. the point at which water has completely reacted with soil CO<sub>2(g)</sub> and carbonates shortly after it entered a closed system (Han et al. 2012). Studied samples have been separated into two groups based on their apparent crossing point which is different for samples in Figures 16 and 17.

Samples in an open system follow the general carbonate dissolution trend confirming that most of the calcite saturation is likely to have occurred in open system conditions (Figure 14). G1 samples that are considered to be in a closed system, orbit around point O in Figure 16, as expected for young water.

Interestingly, although the crossing point seems to have well-defined  $\delta^{13}\text{C}$  and  $^{14}\text{C}$  concentrations for the different sample groups (Figures 16.III and 17.III), two distinct initial DIC concentrations can be identified (point O) (Figures 16.II and 17.II). Samples in Figure 16 reach the crossing point with a DIC concentration approximately 3 times lower (2.3 mmol/L) than those in Figure 17 (7.1 mmol/L) indicating different recharge conditions or an alternate source of DIC for samples in Figure 17. Coincidentally, all samples from Figure 17 (except samples in navy blue) have been identified as having high concentrations of dissolved methane and having undergone some level of microbial methanogenesis (Bordeleau et al. 2015), which would explain the shift in DIC concentrations. Thus age calculations for samples from Figure 17 have to be considered highly uncertain.

On the other hand, most samples from Figure 16 can be assigned geochemical processes that are accounted for by conventional correction methods. Samples identified in green and dark purple, mostly samples from G1, have undergone dissolution of marine carbonates, isotopic exchange between water and soil  $\text{CO}_{2(\text{g})}$  as well as weathering of silicates all under open system conditions. Samples in blue, mostly from G3, have undergone noticeable radiocarbon decay. The sample in orange could have undergone incongruent dissolution of minerals or isotopic exchange between water and carbonate minerals. Samples identified in fuchsia and red, however, lie on the “dead carbon” mixing line (Figure 16.II) and require geochemical modelling. Samples in fuchsia could be the result of the oxidation of fossil organic matter or the weathering of silicates with fossil  $\text{CO}_2$ , both processes requiring long residence times. Finally, samples in red seem to receive a DIC input from methanogenesis involving old organic matter, which is consistent with the fact that these samples were identified to have undergone late stage microbial methanogenesis, suggesting longer residence times (Bordeleau et al. 2015).

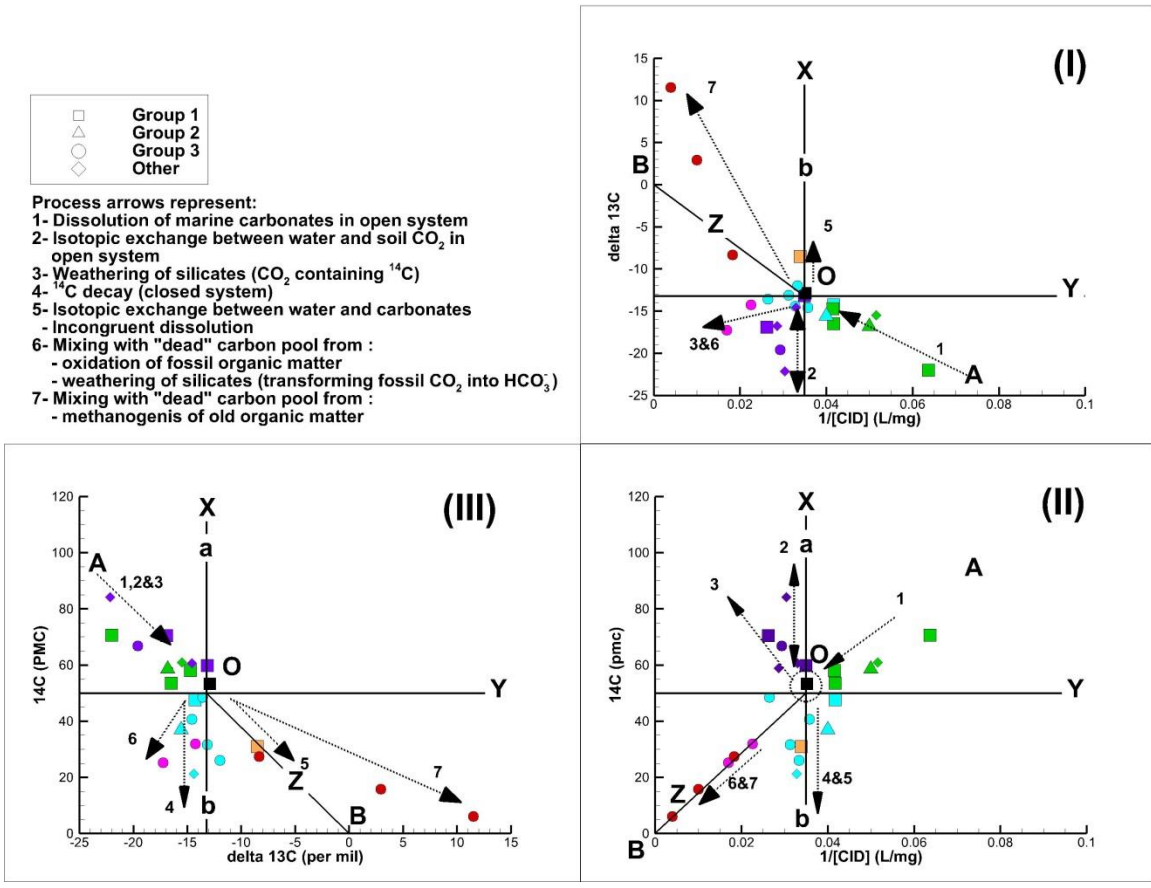


Figure 16 Trends between  $\delta^{13}\text{C}$ ,  $^{14}\text{C}$  and DIC concentrations (Han et al. 2012). Arrows identify geochemical process affecting the samples. Colors identify samples that have undergone similar reactions.

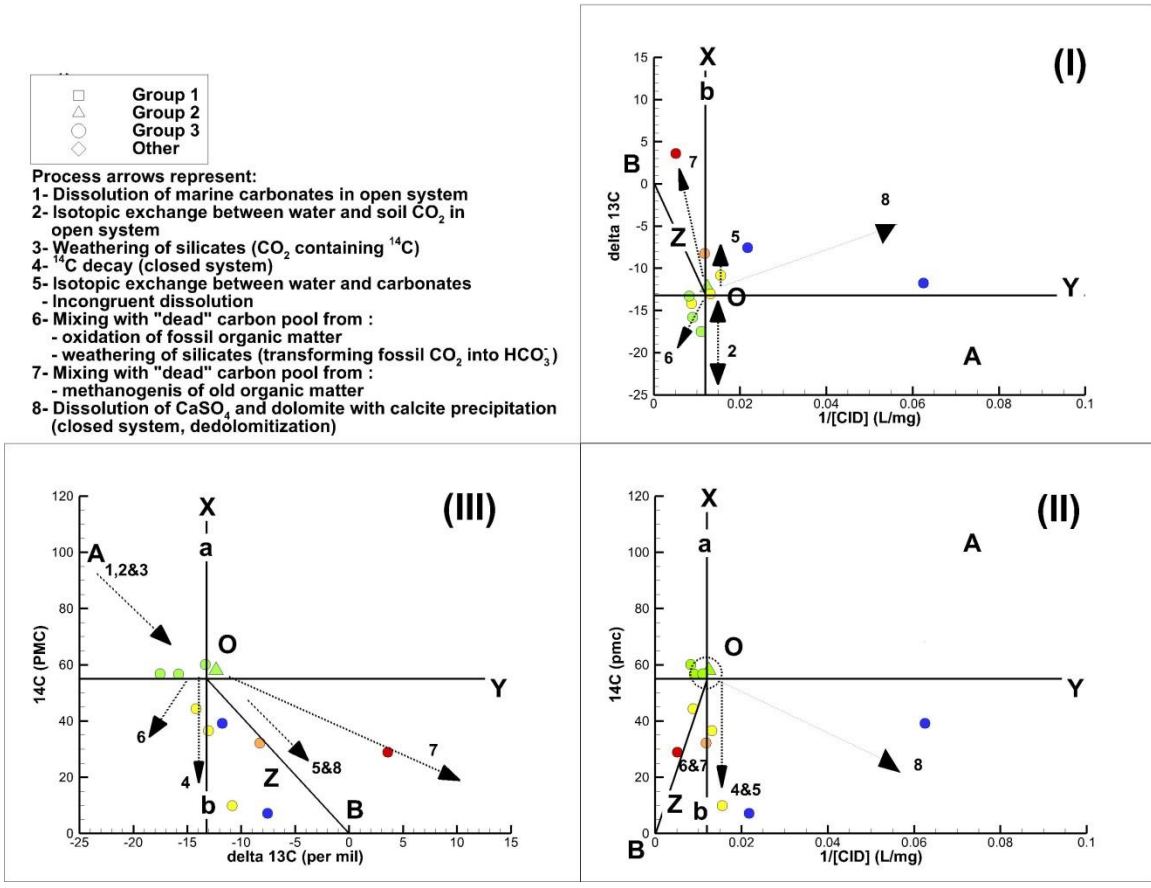


Figure 17 Trends between  $\delta^{13}\text{C}$ ,  $^{14}\text{C}$  and DIC concentration (Han et al. 2012). Arrows identify geochemical process affecting the samples. Colors identify samples that have undergone similar reactions.

## **2.4 Regional Scale Conceptual Model**

The geochemical analysis and the interpretation of the radiocarbon ages of water samples obtained from the study area corroborate and add further insight to the initial regional conceptual flow model hypothesised in Section 2.2 (Figure 18). Most of the groundwater samples had a rapid transit time, thus confirming that flow occurs at shallow depths in the top portion of the fractured rock aquifer where it is under open system conditions with respect to the atmosphere. In the St. Lawrence Lowlands, the piezometric gradients are smaller, leading to slower flow rates which is reflected in water samples showing signs of water freshening even 10 000 years after the retreat of the Champlain Sea . The presence of such waters in shallow residential wells (approximately 60m deep) indicates that the interface between the active flow zone, where the water is rapidly renewed, and slow moving water is close to the surface. Finally, the presence of waters having old ages, long flow paths and possibly mixing with formation brines from the Appalachians, points to the possible existence of a regional flow path emerging near the St. Lawrence River. Overall, the flow system in the Chaudière-Appalaches region seems to follow the Thòthian regional groundwater flow concept (Tòth 1963), which is characterised by nested local, intermediate and regional flow systems.

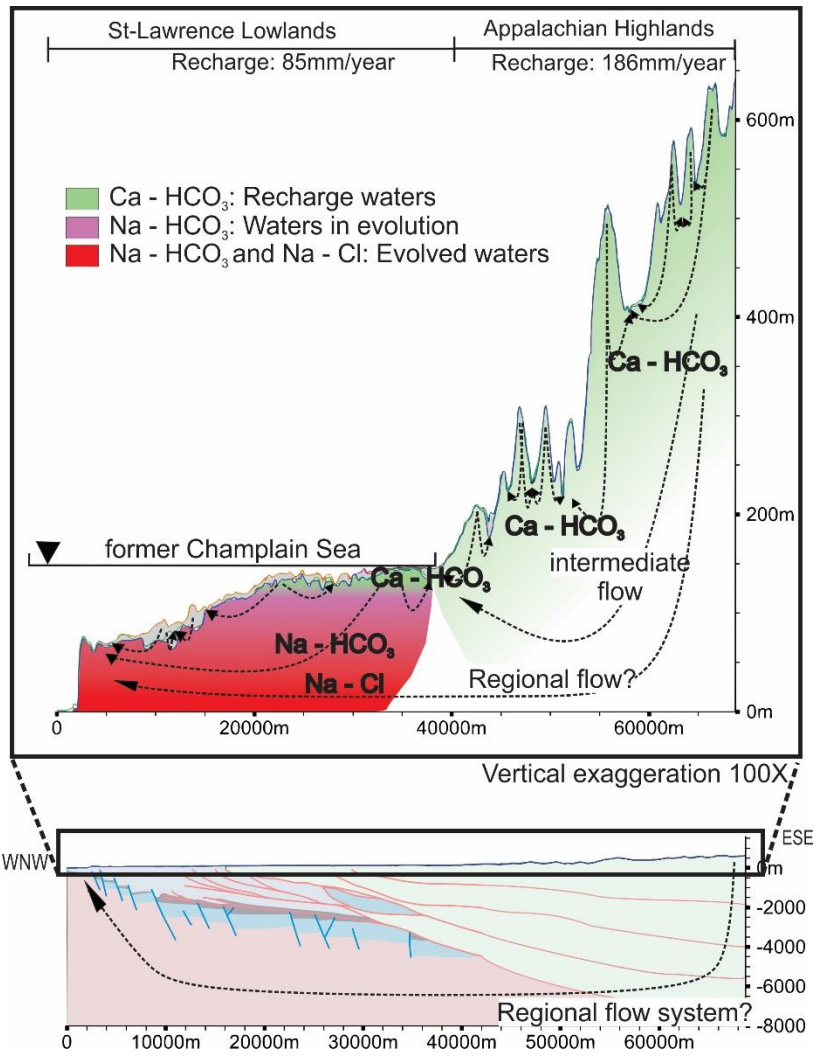


Figure 18 Conceptual regional groundwater flow and geochemical evolution model for the region of Chaudière-Appalaches